

To appear in *The Astronomical Journal*.

Discovery of Radio Outbursts in the Active Nucleus of M81

Luis C. Ho

Carnegie Observatories, 813 Santa Barbara St., Pasadena, CA 91101-1292

Schuyler D. Van Dyk

Infrared Processing and Analysis Center, California Institute of Technology, Mail Code 100-22,
Pasadena, CA 91125

Guy G. Pooley

Mullard Radio Astronomy Observatory, Cavendish Laboratory, Madingley Road, Cambridge,
CB3 0HE, England

Richard A. Sramek

National Radio Astronomy Observatory, P.O. Box 0, Socorro, NM 87801

and

Kurt W. Weiler

Remote Sensing Division, Naval Research Laboratory, Code 7214, Washington, DC 20375-5320

ABSTRACT

The low-luminosity active galactic nucleus of M81 has been monitored at centimeter wavelengths since early 1993 as a by-product of radio programs to study the radio emission from Supernova 1993J. The extensive data sets reveal that the nucleus experienced several radio outbursts during the monitoring period. At 2 and 3.6 cm, the main outburst occurred roughly in the beginning of 1993 September and lasted for approximately three months; at longer wavelengths, the maximum flux density decreases, and the onset of the burst is delayed. These characteristics qualitatively resemble the standard model for adiabatically expanding radio sources, although certain discrepancies between the observations and the theoretical predictions suggest that the model is too simplistic. In addition to the large-amplitude, prolonged variations, we also detected milder changes in the flux density at 3.6 cm and possibly at 6 cm on short ($\lesssim 1$ day) timescales. We discuss a possible association between the radio activity and an optical flare observed during the period that the nucleus was monitored at radio wavelengths.

Subject headings: galaxies: active — galaxies: individual (NGC 3031) — galaxies: nuclei — galaxies: Seyfert — radio continuum: galaxies

1. Introduction

At a distance of only 3.6 Mpc (Freedman et al. 1994), NGC 3031 (M81) hosts perhaps the best studied low-luminosity active galactic nucleus (AGN). Its striking resemblance to “classical” Seyfert 1 nuclei was first noticed by Peimbert & Torres-Peimbert (1981) and Shuder & Osterbrock (1981), and a number of subsequent studies (Filippenko & Sargent 1988; Keel 1989; Ho, Filippenko, & Sargent 1996) have elaborated on its AGN-like characteristics. The nucleus of M81 holds additional significance because of its relevance to a poorly understood class of emission-line objects known as low-ionization nuclear emission-line regions (LINERs: Heckman 1980), whose physical origin is still controversial (Ho 1999 and references therein). The optical classification of the nucleus of M81 borders between LINERs and Seyferts (Ho, Filippenko, & Sargent 1997), but it is clear that the ionization state of its line-emitting regions differs significantly from that of typical Seyfert nuclei (Ho et al. 1996).

The variability properties of low-luminosity AGNs, LINERs in particular, are very poorly known at any wavelength. The faintness of these nuclei renders most observations extremely challenging, and routine monitoring of them has rarely been attempted. M81 remains one of the few LINERs with sufficient data to allow its variability characteristics to be assessed. The occurrence of Supernova (SN) 1993J in late March of 1993 prompted us almost immediately to monitor the supernova interferometrically at radio wavelengths. Since at most wavelengths the field of view of the telescopes contained both the supernova and the center of the galaxy, the observations yielded a useful record of the radio flux density of the nucleus during the period that the supernova was monitored. This paper will examine the radio variability properties of the nucleus of M81 based on these data. We report on the discovery of several radio outbursts, which plausibly could be associated with the optical flare seen by Bower et al. (1996).

2. Radio Observations

The radio data analyzed in this paper are based on observations of SN 1993J made with the Very Large Array (VLA)¹ as reported by Van Dyk et al. (1994), on similar monitoring data acquired using the Ryle Telescope by Pooley & Green (1993), and on unpublished updates to these two data sets since then.

¹The VLA is a facility of the National Radio Astronomy Observatory which is operated by Associated Universities, Inc., under cooperative agreement with the National Science Foundation.

2.1. VLA Data

The VLA data were acquired in snapshot mode at 20 cm (1.4 GHz), 6 cm (4.9 GHz), 3.6 cm (8.4 GHz), 2 cm (14.9 GHz), and 1.3 cm (22.5 GHz), using a 50 MHz bandwidth for each of the two IFs, between 1993 March 31 and 1997 January 23. The different bands were observed nearly simultaneously. As scheduling constraints did not permit us to specify in advance the array configuration for the observations, the data were taken using a mixture of configurations and hence a range of angular resolutions (synthesized beam $0''.25\text{--}44''$). Because of the coarseness of the beam in the most compact configurations and at the longest wavelength, extended, off-nuclear emission can potentially contaminate the signal from the central point source. Inspection of the detailed maps of Kaufman et al. (1996), however, indicates any such contamination of the nucleus, even at 20 cm, is at most a few percent. Since the phase center of the VLA observations was near the position of SN 1993J, and the nucleus of M81 is $2''.64$ from this center, primary beam attenuation had a critical effect on the observations, such that only the 20, 6, and 3.6 cm observations produced reliable data for the nucleus. At 2 cm the nucleus was too close to the edge of the primary beam to produce reliable measurements for all configurations. At 1.3 cm the nucleus was outside the primary beam, and therefore maps were not made of the nucleus at this wavelength.

VLA phase and flux density calibration and data reduction followed standard procedures within the Astronomical Image Processing System (AIPS), such as those described by Weiler et al. (1986), using 3C 286 as the primary flux density calibrator and 1044+719 as the main secondary flux density and phase calibrator. For observations at 20 cm in the more compact D configuration, 0945+664 was the secondary calibrator. The flux density scale is believed to be consistent with that of Baars et al. (1977).

Maps were made of the 20, 6, and 3.6 cm observations in the usual manner within AIPS, offsetting the map center from the observation phase-tracking center to the position of the nucleus. Since the supernova near maximum was nearly as bright as the nucleus (~ 100 mJy), the sidelobes of SN 1993J can severely contaminate the measurements of the nucleus. The size of the map for each frequency and configuration was chosen so that both sources were included in the field, and the map was then deconvolved using the CLEAN algorithm (as implemented in the task IMAGR). We determined the depth of the cleaning by empirically examining the convergence of the recovered flux density. Both the peak and the integrated flux densities of the nucleus on the deconvolved maps were measured by putting a tight box around the source and summing the pixel values using the task IMEAN. Because the nucleus is displaced so far from the phase center, the image of the nucleus is affected at all frequencies by bandwidth smearing, which diminishes the peak flux density relative to the integrated flux density, a conserved quantity. Therefore, we report here only the integrated flux densities. We verified that the more sophisticated procedure of fitting the source with elliptical Gaussians (using the task IMFIT) gives essentially the same results (usually within 3%). The final flux densities were obtained by scaling the observed values with the correction factor for the attenuation of the primary beam. For the 25 m dishes of the

VLA, the correction factors at 20, 6, and 3.6 cm are 1.008, 1.242, and 2.011, respectively, for a phase-center displacement of 2'.64.

Because we are interested in establishing the variability behavior of the nucleus using a data set taken under nonoptimal conditions, it is vital to make a careful assessment of the various sources of uncertainty that can affect the measurements. The following sources of error are considered:

(1) The quality of the maps varies widely, but in general the rms noise in the vicinity of the nucleus ranges from 0.1 to 2 mJy beam⁻¹, with median values of 0.7, 0.3, and 0.4 mJy at 20, 6, and 3.6 cm, respectively. The corresponding fractional error on the total flux densities is 0.8%, 0.4%, and 0.6% at 20, 6, and 3.6 cm, respectively.

(2) As mentioned above, the process of measuring flux densities from the maps itself can introduce an uncertainty as large as ~3%, depending on the method adopted (IMFIT or IMEAN).

(3) The absolute flux density scale of the primary calibrator is assumed accurate to better than 5% (see, e.g., Weiler et al. 1986).

(4) The primary beam of the VLA antennas is accurate only to a few percent at the half power point (Napier & Rots 1982); the exact uncertainty, in fact, has not been determined rigorously (R. Perley and M. Rupen 1999, private communications). For concreteness, we will assume that this source of uncertainty contributes an error of 5% to the primary-beam correction at all frequencies.

(5) Without reference pointing, the VLA can achieve rms pointing errors, under good weather conditions, of 15''–18'' during the night and $\gtrsim 20''$ during the day (Morris 1991). At the half power point of the beam, a pointing error of 20'' results in an amplitude error of 18.4% at 3.6 cm after accounting for primary beam corrections. Assuming that this error is independent among the 27 antennas, we can divide it by $\sqrt{27}$ to get a 3.5% error in the flux measurement of a source at the beam half power point due to pointing. A similar calculation yields an error of 1.3% at 6 cm and 0.09% at 20 cm.

(6) A potentially more serious source of uncertainty comes from systematic pointing errors induced by wind and solar heating; these errors are not expected to be random among the antennas. According to Morris (1991), a wind speed of 8 m s⁻¹ (a typical value for windy conditions) introduces an additional pointing error of ~20''. The formal error due to differential solar heating is difficult to establish because this effect has not been formally quantified for the VLA, but it has been estimated to be a factor of a few smaller than the contribution from moderate winds. We take 20'' as a nominal pointing error for the two contributions. After accounting for primary beam correction, this translates into a flux measurement error of 18% at 3.6 cm, 7% at 6 cm, and 0.5% at 20 cm.

(7) The problem of “beam squint” — the variation of the primary beam caused by slight differences between the pointing centers of the right and left polarizations — is negligible (<0.5%) because we make use only of the total intensity, the sum of both polarizations. We neglect this

contribution to the total error.

A reasonable estimate of the final error budget can be derived by summing in quadrature sources (1) through (5). This corresponds to an uncertainty of approximately 8% for all three frequencies. The true uncertainty of any individual measurement at 3.6 cm, on the other hand, can be substantially larger than this if systematic pointing errors induced by wind or solar heating are significant. In the most extreme situation, the total error could be as large as 20%.

2.2. Ryle Telescope Data

The Ryle Telescope (the upgraded Cambridge 5-km Telescope; Jones 1991) is an E-W synthesis telescope at the time of the observations operating at 15.2 GHz with a bandwidth of 280 MHz. The angular separation between the supernova and the nucleus of M81 places one near the half-power point when the pointing center is at the other. The disk of the galaxy also gives rise to emission on similar angular scales. In order to make a clean distinction between the two responses, and to reject the emission from the disc, we cannot make use of the short baselines (<100 m) in the array: the resolution is inadequate. We therefore use the two groups of longer baselines, near 1.2 and 2.4 km, with interferometer fringe spacings of $2''.6$ and $1''.3$. So long as we avoid the hour angles at which the fringe rates were similar, integration removes the response to any source which is not at the phase center. For the first month after the supernova explosion no observations centered on the nucleus were made; we have not attempted to analyze the data during this interval to derive a flux density for the nucleus. From 1993 May 5 until 1994 June 20, separate pointings were made on the supernova and on the nucleus, together with one on the nearby quasar B0954+658 as a phase calibrator. Amplitude calibration is based on observations of 3C 48 or 3C 286, normally on a daily basis. The data presented here were made with linearly-polarized feeds and are measurements of Stokes I+Q. We estimate that the typical rms uncertainty in the flux densities is $\sim 5\%$. It is apparent from the observations of the phase calibrator, the supernova and the nucleus that some fluctuations in the amplitude scale remain; these are a consequence of poor weather conditions during which the system noise and the gain of the telescope are subject to variations which have not been completely removed by the monitoring systems. As discussed by Pooley & Green (1993), the quasar B0954+658 is strongly variable (a factor of 2 at 15 GHz over the interval covered here), and we fitted a smoothly-varying curve to its apparent flux density in order to reduce the effects of weather and system fluctuations on the results. In retrospect, using a calibrator whose flux density was varying less dramatically would have been better.

3. The Light Curves

The light curves of the nucleus (Fig. 1) exhibit a complex pattern of flux density variations during the monitoring period. The nucleus emits a baseline level of roughly 80–100 mJy at all four

wavelengths, consistent with its historical average (Crane, Giuffrida, & Carlson 1976; de Bruyn et al. 1976; Bietenholz et al. 1996), on which is superposed at least one, and possibly three to four, discrete events during which the flux increased substantially.

The “outbursts” are most clearly visible in the VLA data at 3.6 cm. Although our earliest epoch did not catch the onset of the initial rise of the first event, a local maximum is apparent on day² 13 ± 5 (hereafter outburst “A;” Fig. 1*a*). This outburst reached a peak flux density of 190 mJy, a nearly two-fold increase in brightness over the quiescent state. There is some indication that outburst “A” is present at 6 cm as well; however, it appears to be slightly delayed with respect to 3.6 cm, and the amplitude of the intensity increase compared to the quiescent level is lower, on the order of 40%. We find no convincing evidence for a corresponding variation at 20 cm, and the Ryle observations at 2 cm had not yet begun at this time. The outburst centered near day 200 ± 5 (hereafter “B”) in the 3.6 cm light curve (Fig. 1*b*) has a maximum amplitude of ~ 170 mJy; it can be clearly identified with the 200 mJy peak on day 190 ± 5 at 2 cm, and plausibly with a small maximum near day 205 ± 5 at 6 cm and with the broad peak between days 220–270 at 20 cm. In both of these cases, the amplitude of the variations appear to decrease with increasing wavelength, and the onset of the flares at longer wavelengths seems to be somewhat delayed with respect to the shorter wavelengths. Although the sparse data coverage precludes a detailed temporal analysis, the flares appear to rise and decay on a timescale of 1–2 months. M81 has been monitored only sparsely at the later phases of the program; nonetheless, several additional maxima are evident in the data sets, especially at the two shortest wavelengths, and these might correspond to outbursts similar to “A” and “B.”

In addition to the relatively long-timescale, large-amplitude outbursts, several episodes of rapid variability were imprinted in the densely sampled portion of the 3.6 cm light curve during the first two months (Fig. 1*a*). The source brightness flickers by 30%–60% on a timescale of a day or less, which implies that the emission originates from regions with dimensions $\lesssim 0.001$ pc. Note that the amplitude of the short-term variability is significantly larger than the measurement uncertainty, even after allowing for pointing errors induced by strong winds (see § 2.1). Crane et al. (1976) previously discussed rapid variability of a similar, perhaps somewhat less extreme, nature in M81 at this wavelength. They found the nucleus to vary by about 40% in the course of a week. Corresponding variations at longer wavelengths are less apparent; at 6 cm, rapid fluctuations occur at most at a level of $\sim 10\%$, and none are significant at 20 cm.

The wavelength dependent variations in flux density naturally lead to strong spectral variations during the outbursts. Figure 2 displays the time variation of the spectral index, α , defined such that $S_\nu \propto \nu^\alpha$, where S_ν is the flux density at frequency ν . As has been well established (de Bruyn et al. 1976; Bartel et al. 1982; Reuter & Lesch 1996), the M81 radio core during quiescence has a flat to slightly inverted spectrum; we measure $\alpha \approx 0$ to $+0.3$ from 2 to

²The light curves will be referenced to days since 1993 March 28.0 UT, the adopted date of the explosion of SN 1993J.

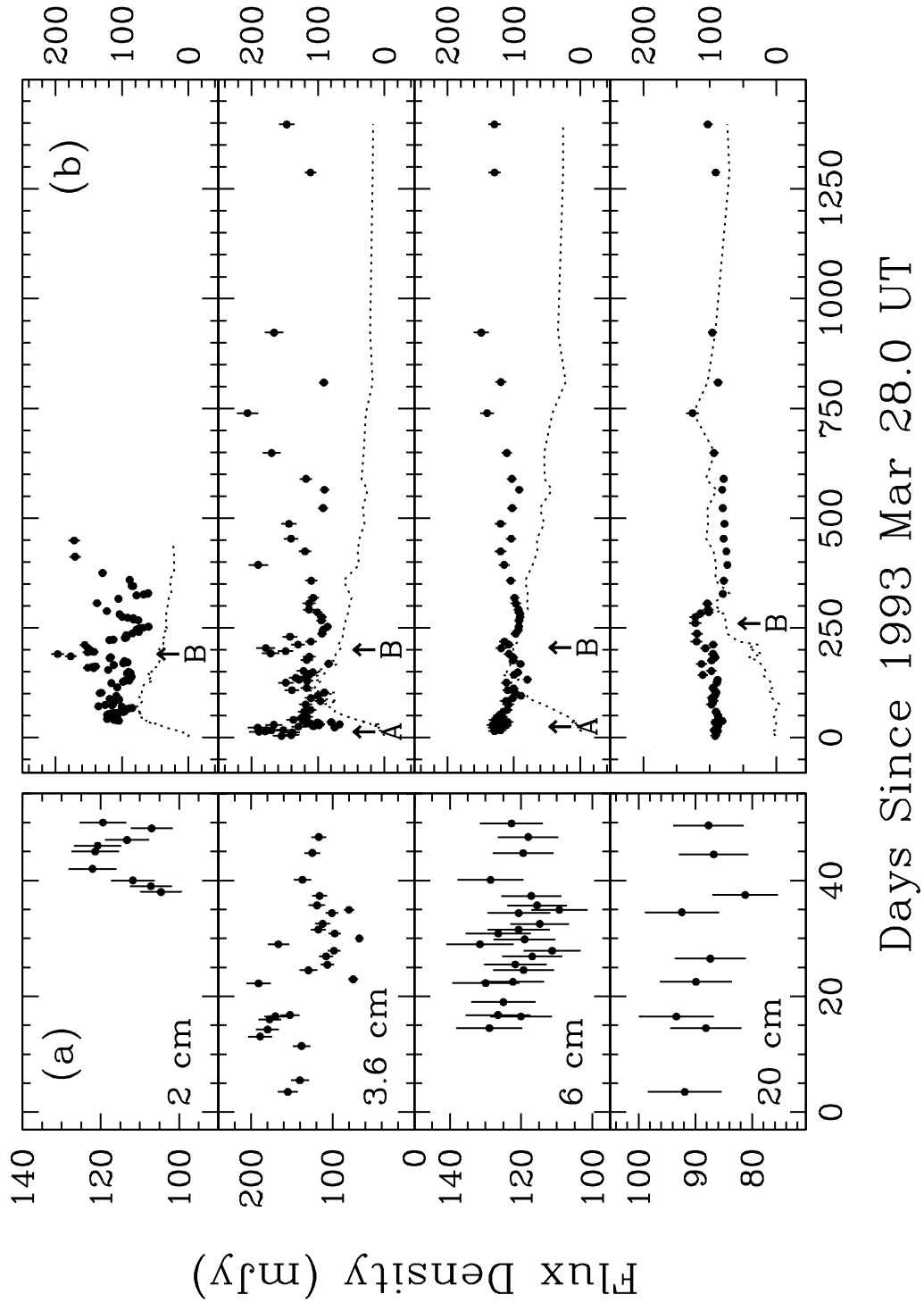


Fig. 1.— Radio light curves of the nucleus of M81. The abscissa denotes days since the explosion of SN 1993J, which we adopt as 1993 March 28.0 UT. The flux densities for the first 55 days (a) are shown separately from the full data set (b) in order to highlight the short timescale variations discernible in the closely-sampled part of the light curve. The dashed lines represent the light curves of SN 1993J measured from the same images. Outbursts A and B are marked with arrows.

20 cm, consistent with previous determinations.

We are convinced that the variations in flux density with time of the nucleus are real and intrinsic to the source. The dotted lines in Figure 1*b* trace the observed light curves of SN 1993J as derived from the same images from which we measured the nucleus. The supernova light curves exhibit no unusual behavior and are well represented by the model of the emission discussed in Van Dyk et al. (1994). The flux and phase calibrations are therefore reliable, and we cannot attribute the changes in the source to unsuspected variability in the calibrators. The effect of sidelobe contamination by the supernova should not be significant, as SN 1993J is no stronger than the nucleus, and, moreover, the sidelobes are greatly reduced in the cleaned maps. In the case of the VLA data, we have properly corrected for primary-beam attenuation, we have taken into account the effects of bandwidth smearing, and we have carefully considered all known sources of errors affecting the flux density measurements. The only source of uncertainty we did not include formally into our error budget is that potentially arising from systematic pointing errors induced by wind and solar heating (see § 2.1). However, we believe that the main outbursts cannot be attributed to systematic errors for the following reasons. First, the observed variations are much larger than even the most pessimistic error estimate. Second, the main outbursts are clearly well resolved in time and so do not arise from any single, errant data point. And finally, one of the outbursts is seen both in the VLA *and* in the Ryle data sets, which implies that it cannot be attributed to artifacts of primary-beam correction of the VLA data. We further note that the variations cannot be a configuration-related effect, since the flux densities, particularly at 3.6 cm, do not achieve the same level of variation for observations made in the same array configuration but separated in time.

4. The Radio Variability and Its Implications

Previous radio work by Crane et al. (1976) and de Bruyn et al. (1976) showed that the nucleus of M81 undergoes gradual flux variations over several years, accompanied by erratic changes on much shorter timescales. Moreover, these authors recorded the onset of a flare in 1974 October; the flux density at 8085 MHz increased by $\sim 40\%$ over one week. The limited time coverage did not permit the entire event to be monitored, however, although simultaneous observations at 2695 MHz suggested that the flux enhancement might have occurred first at the higher frequency. Similarly, Kaufman et al. (1996) suggested that a modest flare at 6 cm possibly occurred during 1981 August. The observations presented in this paper establish conclusively that the nucleus of M81 is strongly variable at centimeter wavelengths. Our time coverage enabled us to identify rapid variability on timescales as short as one day or less at 3.6 cm, and more spectacularly, two distinctive outbursts which could be traced in more than one wavelength, as well as several others seen in at least one of the shorter wavelengths monitored.

Several properties of the best-defined outburst (“B”), namely the steep rise and decline of the light curve, and the frequency dependence of the burst onset and the burst maximum, suggest that

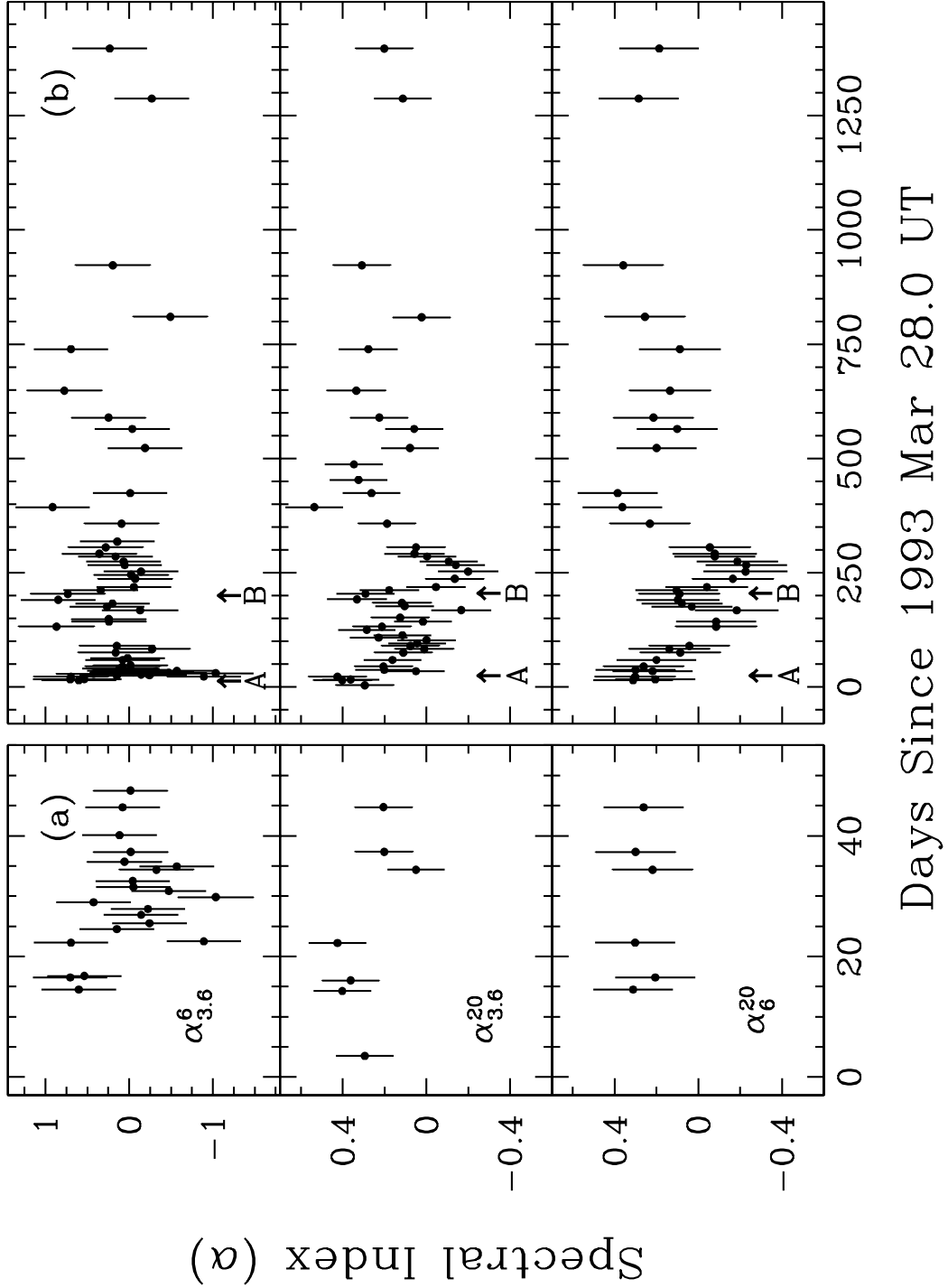


Fig. 2.— Variation in the radio spectral index α , where $S_\nu \propto \nu^\alpha$. Three indices are shown: $\alpha_{3.6}^6 = \alpha$ between 6 and 3.6 cm; $\alpha_{3.6}^{20} = \alpha$ between 20 and 3.6 cm; and $\alpha_6^{20} = \alpha$ between 20 and 6 cm. The data for the first 55 days (a) are shown separately from the full data set (b). Outbursts A and B are marked with arrows.

the standard adiabatic-expansion model for variable radio sources (Pauliny-Toth & Kellermann 1966; van der Laan 1966) may be applicable. This model idealizes the radio flux variability as arising from an instantaneous injection of a cloud of relativistic electrons which is uniform, spherical, and expanding at a constant velocity. The flux density increases with source radius (or time) while the source remains optically thick, and it decreases during the optically thin phase of the expansion. Both the maximum flux density and the frequency at which it occurs decrease with time. The observed characteristics of outburst “B”, however, do not agree in detail with the predictions of this simple model, as is also the case for other variable radio sources (see discussion in Kellermann & Owen 1988). In particular, the observed profile of the burst at 2 and 3.6 cm is much shallower than predicted; it follows roughly a linear rise and a linear decline, whereas an adiabatically expanding source should brighten as t^3 before the maximum and, for electrons having a power-law energy distribution with a slope of -2.5 , decline thereafter as t^{-5} . Moreover, the 3.6 and 6 cm peaks occur much earlier than expected relative to the 2 cm peak, and the relative strengths of the peaks do not follow the predicted scaling relations. These inconsistencies no doubt reflect the oversimplification of the standard model. Realistic modeling of the M81 source, which is beyond the scope of this work, most likely will need to incorporate more complex forms of the particle injection rate (see, e.g., Peterson & Dent 1973), as well as departures from spherical symmetry, since the radio source is known to have an elongated geometry, plausibly interpreted as a core-jet structure (Bartel et al. 1982; Bartel, Bietenholz, & Rupen 1995; Bietenholz et al. 1996; Ebberts et al. 1998). The nuclear jet model of Falcke (1996), for instance, can serve as a useful starting point.

It is instructive to consider whether the radio variability in M81 is associated with any other visible signs of transient activity, at either radio or other wavelengths, during the monitoring period. By analogy with other accretion-powered systems, such as Galactic superluminal sources (see, e.g., Harmon et al. 1997), one might expect the radio outbursts in the M81 nucleus to be accompanied by detectable changes in its radio structure and to be preceded by X-ray flares. The nucleus has been intensively imaged at milli-arcsec resolution in concert with VLBI studies of SN 1993J. Bietenholz, Bartel, & Rupen (1998) and Ebberts et al. (1998) do, in fact, report structural changes in the jet component of the nucleus at 3.6 cm on timescales of weeks, although the limited VLBI data do not permit a direct comparison with our VLA light curves. Several measurements of the nuclear flux in the hard X-ray band (2–10 keV) were taken by *ASCA* between 1993 May and 1995 April (Ishisaki et al. 1996), but again, because of the limited temporal coverage, these data cannot be used to draw any meaningful comparisons with the radio light curve.

We mention, however, a possible connection between the radio outbursts and an optical flare that was caught during the same monitoring period. After 15 years of relative constancy (Ho et al. 1996), the broad $H\alpha$ emission line of the nucleus of M81 brightened by $\sim 40\%$ and developed a pronounced double-peaked line profile (Bower et al. 1996) reminiscent of those seen in a minority of AGNs (Eracleous & Halpern 1994 and references therein). Neither the exact date of its onset nor its time evolution is known, except that it occurred between 1993 April 14 (when it was last

observed by Ho et al.) and 1995 March 22 (the date of Bower et al.’s observations), within the period of the radio monitoring. The physical origin of double-peaked broad emission lines in AGNs is not yet fully understood (see Halpern et al. 1996 for a discussion), and the detection of possibly related variable radio emission does not offer a clear discriminant between the main competing models. Nevertheless, the association of the sudden appearance of the double-peaked line with another transient event, namely the radio outbursts, hints that the two events could have a common origin. Both phenomena, for example, at least in this case, may originate from a sudden increase in the accretion rate.

Finally, we note that radio outbursts may be a generic property of low-luminosity AGNs, especially those classified as LINERs. Although no other nearby LINER has had its variability properties scrutinized to the same degree as M81, radio flares have been noticed in at least three other famous LINER nuclei. NGC 1052 is known to have experienced two outbursts at millimeter wavelengths (Heeschen & Puschell 1983) and another at longer wavelengths (Slee et al. 1994). A single outburst at centimeter wavelengths has been reported for the nucleus of M87 (Morabito, Preston, & Jauncey 1988). And Wrobel & Heeschen (1991) remark that NGC 4278 exhibited pronounced variability at 6 cm over the course of 1–2 years. In this regard, it is appropriate to mention that even the extremely low-power radio source in the center of the Milky Way, Sgr A*, showcases outbursts at high radio frequencies (Zhao et al. 1992; Wright & Backer 1993). The radio variability characteristics of these weak nuclei closely mimic those of far more powerful radio cores traditionally studied in quasars and radio galaxies, and they furnish additional evidence that the AGN phenomenon spans an enormous range in luminosity.

5. Summary

We analyzed the radio light curves of the low-luminosity active nucleus in the nearby spiral galaxy M81 taken at 3.6, 6, and 20 cm over a four-year period between 1993 and 1997, as well as a 2 cm light curve covering a more limited span between 1993 and 1994. Two types of variability are seen: rapid ($\lesssim 1$ day), small-amplitude (10%–60%) flux density changes are evident at 3.6 and 6 cm, and at least one, and possibly three or four longer timescale (months), outbursts of greater amplitude (30%–100%). The best observed of the outbursts can be traced in three bands. The maximum flux density decreases systematically with decreasing frequency, and the time at which the maximum occurs is shifted toward later times at lower frequencies. These characteristics qualitatively agree with the predictions of the adiabatic-expansion model for variable radio sources, although certain discrepancies between the observations and the model predictions suggest that the model needs to be refined. The radio outbursts may be related to an optical flare during which the broad H α emission line developed a double-peaked structure. Although the exact relationship between the two events is unclear, both phenomena may stem from a sudden increase in the accretion rate.

During the course of this work, L. C. H. was supported by a postdoctoral fellowship from the Harvard-Smithsonian Center for Astrophysics, by NASA grant NAG 5-3556, and by NASA grants GO-06837.01-95A and AR-07527.02-96A from the Space Telescope Science Institute (operated by AURA, Inc., under NASA contract NAS5-26555). K. W. W. wishes to acknowledge the Office of Naval Research for the 6.1 funding which supports his work. We thank Norbert Bartel, Michael Eracleous, Heino Falcke, and the referee for helpful comments, and Rick Perley and Michael Rupen for advice concerning pointing errors of the VLA.

A. The Data

For the sake of completeness, we list in Tables 1–4 the flux densities of the nucleus of M81. The uncertainties in the flux densities were calculated as described in § 2.1. These are the data plotted in Figure 1.

TABLE 1
FLUX DENSITIES OF THE NUCLEUS AT 2 CM

UT Date	Day ^a	S_ν (mJy)	σ (mJy)	UT Date	Day ^a	S_ν (mJy)	σ (mJy)
1993 May 05.29	38.29	104.6	5.2	1993 Sep 04.85	161.85	144.3	7.2
1993 May 06.29	39.29	107.2	5.4	1993 Sep 05.98	162.98	139.8	7.0
1993 May 07.29	40.29	111.8	5.6	1993 Sep 09.09	165.09	112.6	5.6
1993 May 09.28	42.28	122.1	6.1	1993 Sep 13.09	169.09	98.2	4.9
1993 May 12.21	45.21	121.4	6.1	1993 Sep 14.99	171.99	91.7	4.6
1993 May 13.24	46.24	120.8	6.0	1993 Sep 17.83	174.83	96.4	4.8
1993 May 14.23	47.23	113.3	5.7	1993 Sep 24.84	181.84	118.2	5.9
1993 May 16.20	49.20	107.0	5.3	1993 Sep 26.80	183.80	116.9	5.8
1993 May 17.19	50.19	119.4	6.0	1993 Sep 29.12	185.12	177.0	8.8
1993 May 19.26	52.26	122.4	6.1	1993 Oct 04.00	190.00	196.9	9.8
1993 May 21.20	54.20	119.7	6.0	1993 Oct 07.81	194.81	151.6	7.6
1993 May 22.20	55.20	115.9	5.8	1993 Oct 08.77	195.77	142.3	7.1
1993 May 23.20	56.20	111.8	5.6	1993 Oct 10.09	196.09	144.4	7.2
1993 May 24.30	57.30	105.5	5.3	1993 Oct 15.76	202.76	149.9	7.5
1993 May 25.10	58.10	98.2	4.9	1993 Oct 25.06	211.06	156.0	7.8
1993 May 26.10	59.10	95.9	4.8	1993 Nov 04.76	222.76	119.1	6.0
1993 Jun 01.22	65.22	96.3	4.8	1993 Nov 05.71	223.71	113.2	5.7
1993 Jun 02.12	66.12	89.3	4.5	1993 Nov 09.73	227.73	95.8	4.8
1993 Jun 03.07	67.07	84.7	4.2	1993 Nov 10.72	228.72	93.4	4.7
1993 Jun 06.21	70.21	100.4	5.0	1993 Nov 15.90	233.90	93.6	4.7
1993 Jun 07.35	71.35	135.4	6.8	1993 Nov 19.67	237.67	84.6	4.2
1993 Jun 09.20	73.20	115.2	5.8	1993 Nov 22.56	240.56	74.7	3.7
1993 Jun 10.20	74.20	125.6	6.3	1993 Nov 28.95	246.95	78.3	3.9
1993 Jun 13.19	77.19	113.0	5.6	1993 Nov 30.76	248.76	74.9	3.7
1993 Jun 20.09	84.09	110.7	5.5	1993 Dec 01.64	249.64	73.4	3.7
1993 Jun 21.07	85.07	112.4	5.6	1993 Dec 02.64	250.64	68.3	3.4
1993 Jun 22.10	86.10	104.4	5.2	1993 Dec 04.64	252.64	59.8	3.0
1993 Jun 22.96	87.96	104.5	5.2	1993 Dec 05.63	253.63	60.4	3.0
1993 Jun 24.27	88.27	118.6	5.9	1993 Dec 19.65	267.65	75.4	3.8
1993 Jul 01.14	95.14	108.4	5.4	1993 Dec 21.60	269.60	82.7	4.1
1993 Jul 07.32	101.32	133.2	6.7	1993 Dec 24.59	272.59	83.0	4.1
1993 Jul 08.16	102.16	131.2	6.6	1993 Dec 26.43	273.43	91.5	4.6
1993 Jul 20.05	114.05	107.2	5.4	1993 Dec 28.43	275.43	99.5	5.0
1993 Jul 29.88	124.88	116.0	5.8	1994 Jan 02.57	281.57	103.7	5.2
1993 Aug 02.24	127.24	98.5	4.9	1994 Jan 09.62	288.62	122.8	6.1
1993 Aug 04.25	129.25	96.3	4.8	1994 Jan 28.36	306.36	137.5	6.9
1993 Aug 04.84	130.84	89.1	4.5	1994 Feb 07.32	316.32	105.2	5.3
1993 Aug 12.82	138.82	85.9	4.3	1994 Feb 15.30	324.30	78.2	3.9
1993 Aug 14.23	139.23	85.6	4.3	1994 Feb 17.40	326.40	67.5	3.4
1993 Aug 16.22	141.22	88.6	4.4	1994 Feb 19.46	328.46	61.1	3.1
1993 Aug 19.95	145.95	89.9	4.5	1994 Feb 20.46	329.46	60.6	3.0
1993 Aug 20.91	146.91	92.7	4.6	1994 Mar 07.68	345.68	82.9	4.1
1993 Aug 22.21	147.21	87.3	4.4	1994 Mar 08.30	345.30	85.2	4.3
1993 Aug 24.99	150.99	90.0	4.5	1994 Mar 21.50	359.50	88.6	4.4
1993 Aug 29.19	154.19	120.7	6.0	1994 Apr 07.20	375.20	129.2	6.5
1993 Sep 01.89	158.89	142.6	7.1	1994 May 14.07	412.07	170.6	8.5
1993 Sep 02.83	159.83	151.4	7.6	1994 Jun 20.10	449.10	172.0	8.6

^aDays since 1993 March 28.0 UT, the adopted date for the explosion of SN 1993J.

TABLE 2
FLUX DENSITIES OF THE NUCLEUS AT 3.6 CM

UT Date	Day ^a	S_ν (mJy)	σ (mJy)	UT Date	Day ^a	S_ν (mJy)	σ (mJy)
1993 Mar 31.10	3.10	154.8	12.2	1993 Aug 10.93	135.93	133.4	10.5
1993 Apr 02.30	5.30	140.0	11.0	1993 Aug 12.92	137.92	117.5	9.3
1993 Apr 08.42	11.42	138.1	10.9	1993 Aug 17.78	142.78	113.9	9.0
1993 Apr 10.06	13.06	188.7	14.9	1993 Aug 23.50	148.50	107.6	8.5
1993 Apr 11.27	14.27	179.7	14.1	1993 Aug 26.93	151.93	121.7	9.6
1993 Apr 13.02	16.02	177.2	14.0	1993 Sep 11.91	167.91	83.8	6.8
1993 Apr 13.54	16.54	170.0	13.4	1993 Sep 18.81	176.81	116.8	9.2
1993 Apr 14.04	17.04	152.2	12.0	1993 Sep 26.74	183.74	112.9	8.9
1993 Apr 19.22	22.22	190.7	15.0	1993 Oct 04.66	191.66	171.2	13.5
1993 Apr 19.94	22.94	74.8	5.9	1993 Oct 10.80	196.80	148.8	11.7
1993 Apr 21.49	24.49	129.5	10.2	1993 Oct 17.79	203.79	178.6	14.1
1993 Apr 22.47	25.47	106.4	8.4	1993 Oct 25.60	211.60	130.0	10.2
1993 Apr 23.89	26.89	108.0	8.5	1993 Nov 01.58	218.58	110.7	8.8
1993 Apr 24.87	27.87	98.3	7.8	1993 Nov 12.64	229.64	142.2	11.2
1993 Apr 25.99	28.99	166.3	13.1	1993 Nov 19.58	236.58	93.9	7.4
1993 Apr 26.85	29.85	67.3	5.4	1993 Nov 28.55	245.55	92.0	7.2
1993 Apr 27.84	30.84	97.3	7.7	1993 Dec 05.57	252.57	85.6	6.7
1993 Apr 28.52	31.52	117.4	9.2	1993 Dec 19.57	266.57	94.9	7.5
1993 Apr 29.50	32.50	112.1	8.8	1993 Dec 27.55	274.55	94.2	7.4
1993 May 01.37	34.37	100.9	7.9	1994 Jan 07.36	285.36	100.9	7.9
1993 May 01.93	34.93	79.9	6.3	1994 Jan 13.48	291.48	113.5	8.9
1993 May 02.71	35.71	119.1	9.4	1994 Jan 27.29	305.29	113.4	8.9
1993 May 04.35	37.35	116.0	9.1	1994 Feb 09.21	318.21	107.1	8.4
1993 May 07.12	40.12	137.1	10.8	1994 Mar 20.34	357.34	110.1	8.7
1993 May 11.75	44.75	124.8	9.9	1994 Apr 25.18	393.18	189.9	15.0
1993 May 14.20	47.20	117.0	9.2	1994 May 26.16	424.16	119.4	9.4
1993 May 25.98	58.98	120.9	9.5	1994 Jun 23.98	452.98	140.5	11.1
1993 May 30.04	63.04	111.1	8.8	1994 Jul 28.00	487.00	143.7	11.3
1993 Jun 11.06	75.06	118.5	9.3	1994 Sep 01.69	522.69	92.4	7.3
1993 Jun 18.92	82.92	96.3	7.8	1994 Oct 13.63	564.63	90.1	7.2
1993 Jun 25.72	89.72	110.6	8.7	1994 Nov 07.47	589.47	118.0	9.3
1993 Jul 01.22	95.22	100.3	7.9	1995 Jan 05.39	648.39	169.7	13.4
1993 Jul 08.76	102.76	90.3	7.3	1995 Apr 06.14	739.14	206.0	16.2
1993 Jul 13.78	107.78	139.2	11.1	1995 Jun 15.00	809.00	91.2	7.2
1993 Jul 19.01	113.01	116.9	9.2	1995 Oct 06.66	922.66	166.1	13.1
1993 Jul 30.88	124.88	148.3	11.7	1996 Oct 05.57	1287.57	111.3	8.8
1993 Aug 04.00	129.00	116.2	9.3	1997 Jan 23.18	1397.18	147.0	11.6
1993 Aug 06.94	131.94	128.6	10.2				

TABLE 3
FLUX DENSITIES OF THE NUCLEUS AT 6 CM

UT Date	Day ^a	S_ν (mJy)	σ (mJy)	UT Date	Day ^a	S_ν (mJy)	σ (mJy)
1993 Apr 11.25	14.25	128.9	9.3	1993 Aug 06.95	131.95	79.7	5.8
1993 Apr 13.51	16.51	120.0	8.7	1993 Aug 17.79	142.79	99.7	7.2
1993 Apr 14.06	17.06	126.5	9.1	1993 Aug 23.50	148.50	94.1	6.8
1993 Apr 16.01	19.01	125.0	9.0	1993 Sep 11.91	167.91	90.1	6.7
1993 Apr 19.28	22.28	129.9	9.4	1993 Sep 19.75	175.75	101.0	7.3
1993 Apr 20.00	23.00	122.3	8.8	1993 Sep 26.74	182.74	101.2	7.3
1993 Apr 21.53	24.53	119.3	8.6	1993 Oct 04.66	190.66	107.3	7.8
1993 Apr 22.50	25.50	121.6	8.8	1993 Oct 17.79	203.79	119.1	8.6
1993 Apr 23.89	26.89	116.9	8.4	1993 Oct 25.61	211.61	107.8	7.8
1993 Apr 24.86	27.86	111.3	8.0	1993 Nov 01.58	218.58	114.2	8.3
1993 Apr 25.98	28.98	131.6	9.5	1993 Nov 19.58	236.58	97.6	7.0
1993 Apr 26.83	29.83	119.0	8.7	1993 Nov 28.56	245.56	93.2	6.7
1993 Apr 27.83	30.83	126.4	9.1	1993 Dec 05.58	252.58	92.5	6.7
1993 Apr 28.50	31.50	120.7	8.7	1993 Dec 19.58	266.58	92.1	6.6
1993 Apr 29.49	32.49	114.8	8.3	1993 Dec 27.56	274.56	90.7	6.5
1993 May 01.36	34.36	120.7	8.7	1994 Jan 07.37	285.37	92.3	6.7
1993 May 01.92	34.92	109.3	7.9	1994 Jan 13.50	291.50	93.2	6.7
1993 May 02.70	35.70	115.5	8.4	1994 Jan 27.29	305.29	97.1	7.0
1993 May 04.33	37.33	117.1	8.5	1994 Feb 09.21	318.21	99.0	7.1
1993 May 07.10	40.10	128.6	9.3	1994 Mar 20.38	357.38	104.7	7.6
1993 May 11.72	44.72	119.4	8.6	1994 Apr 25.18	393.18	114.6	8.3
1993 May 14.17	47.17	118.0	8.5	1994 May 26.19	424.19	120.1	8.7
1993 May 16.85	49.85	122.7	8.9	1994 Jun 23.98	452.98	104.1	7.5
1993 May 25.99	58.99	115.8	8.4	1994 Jul 28.03	487.03	120.2	8.7
1993 May 30.04	63.04	109.9	7.9	1994 Sep 01.68	522.68	102.6	7.4
1993 Jun 11.06	75.06	108.4	7.8	1994 Oct 13.63	564.63	91.9	6.7
1993 Jun 18.93	82.93	112.0	8.1	1994 Nov 07.47	589.47	103.0	7.4
1993 Jun 25.75	89.75	101.9	7.3	1995 Jan 05.39	648.39	110.6	8.0
1993 Jul 01.21	95.21	89.2	6.5	1995 Apr 06.13	739.13	140.3	10.1
1993 Jul 08.76	102.76	98.8	7.2	1995 Jun 16.08	810.08	119.6	8.6
1993 Jul 13.77	107.77	109.4	7.9	1995 Oct 06.71	922.71	149.1	10.8
1993 Jul 19.01	112.01	100.4	7.2	1996 Oct 05.55	1287.55	129.0	9.3
1993 Jul 30.87	124.87	111.2	8.1	1997 Jan 23.24	1397.24	129.3	9.3

^aDays since 1993 March 28.0 UT, the adopted date for the explosion of SN 1993J.

TABLE 4
FLUX DENSITIES OF THE NUCLEUS AT 20 CM

UT Date	Day ^a	S_ν (mJy)	σ (mJy)	UT Date	Day ^a	S_ν (mJy)	σ (mJy)
1993 Mar 31.10	3.10	91.9	6.5	1993 Oct 17.78	203.78	106.6	7.7
1993 Apr 11.29	14.29	88.1	6.3	1993 Oct 25.59	211.59	95.0	7.2
1993 Apr 14.06	17.06	93.4	6.6	1993 Nov 01.56	218.56	120.0	9.1
1993 Apr 19.98	22.98	89.9	6.4	1993 Nov 19.56	236.56	119.3	8.8
1993 Apr 23.87	26.87	87.3	6.2	1993 Dec 05.56	260.56	121.8	9.5
1993 May 01.90	34.90	92.4	6.5	1993 Dec 19.56	274.56	121.8	9.0
1993 May 04.38	37.38	81.2	5.8	1993 Dec 27.54	282.54	113.9	8.3
1993 May 11.77	44.77	86.8	6.2	1994 Jan 07.35	285.35	101.6	7.4
1993 May 16.84	49.84	87.7	6.2	1994 Jan 13.48	291.48	102.6	8.0
1993 May 25.97	58.97	90.7	6.4	1994 Jan 27.27	305.27	103.8	7.5
1993 Jun 11.03	75.03	97.5	6.9	1994 Feb 18.31	327.31	80.5	5.7
1993 Jun 18.88	82.88	94.6	6.8	1994 Mar 20.39	357.39	78.9	5.6
1993 Jun 25.72	89.72	96.7	6.9	1994 Apr 25.17	393.17	73.6	5.2
1993 Jul 01.19	95.19	92.9	6.6	1994 May 26.13	424.13	75.0	5.3
1993 Jul 08.73	102.73	90.4	6.4	1994 Jun 23.97	452.97	79.1	5.6
1993 Jul 13.74	107.74	93.0	6.6	1994 Jul 27.98	486.98	77.8	5.6
1993 Jul 18.99	112.99	95.5	6.8	1994 Sep 01.67	522.67	80.4	5.7
1993 Jul 30.84	124.84	89.6	6.3	1994 Oct 13.62	564.62	81.3	5.9
1993 Aug 06.93	131.93	88.3	6.3	1994 Nov 07.46	589.46	79.2	5.6
1993 Aug 17.77	142.77	110.6	7.9	1995 Jan 05.38	648.38	93.8	6.9
1993 Aug 26.92	151.92	97.5	7.0	1995 Apr 06.12	739.12	126.1	9.4
1993 Sep 11.90	167.90	112.6	8.5	1995 Jun 16.09	809.09	87.6	6.2
1993 Sep 19.73	175.73	97.2	7.1	1995 Oct 06.72	922.72	96.2	6.8
1993 Sep 26.72	182.72	91.9	6.7	1996 Oct 05.52	1287.52	91.1	6.5
1993 Oct 04.65	190.65	95.2	7.3	1997 Jan 23.21	1397.21	102.9	7.3

^aDays since 1993 March 28.0 UT, the adopted date for the explosion of SN 1993J.

References

- Baars, J. W. M., Genzel, R., Pauliny-Toth, I. I. K., & Witzel, A., 1977, *A&A*, 61, 99
- Bartel, N., et al. 1982, *ApJ*, 262, 556
- Bartel, N., Bietenholz, M. F., & Rupen, M. P. 1995, in *Proc. Natl. Acad. Sci.*, 92, 11374
- Bietenholz, M. F., et al. 1996, *ApJ*, 457, 604
- Bietenholz, M. F., Bartel, N., & Rupen, N. P. 1998, in *IAU Colloq. 164, Radio Emission from Galactic and Extragalactic Compact Sources*, ed. A. Zensus, G. Taylor, & J. Wrobel (San Francisco: ASP), 201
- Bower, G. A., Wilson, A. S., Heckman, T. M., & Richstone, D. O. 1996, *AJ*, 111, 1901
- Crane, P. C., Giuffrida, B., & Carlson, J. B. 1976, *ApJ*, 203, L113
- de Bruyn, A. G., Crane, P. C., Price, R. M., & Carlson, J. 1976, *A&A*, 46, 243
- Ebbers, A., Bartel, N., Bietenholz, M. F., Rupen, N. P., & Beasley, A. J. 1998, in *IAU Colloq. 164, Radio Emission from Galactic and Extragalactic Compact Sources*, ed. A. Zensus, G. Taylor, & J. Wrobel (San Francisco: ASP), 203
- Eracleous, M., & Halpern, J. P. 1994, *ApJS*, 90, 1
- Falcke, H. 1996, *ApJ*, 464, L67
- Filippenko, A. V., & Sargent, W. L. W. 1988, *ApJ*, 324, 134
- Freedman, W. L., et al. 1994, *ApJ*, 427, 628
- Halpern, J. P., Eracleous, M., Filippenko, A. V., & Chen, K. 1996, *ApJ*, 464, 704
- Harmon, B. A., Deal, K. J., Paciesas, W. S., Zhang, S. N., Robinson, C. R., Gerard, E., Rodríguez, L. F., & Mirabel, I. F. 1997, *ApJ*, 477, L85
- Heckman, T. M. 1980, *A&A*, 87, 152
- Heeschen, D. S., & Puschell, J. J. 1983, *ApJ*, 267, L11
- Ho, L. C. 1999, in *The AGN-Galaxy Connection*, ed. H. R. Schmitt, L. C. Ho, & A. L. Kinney (Advances in Space Research), in press (astro-ph/9807273)
- Ho, L. C., Filippenko, A. V., & Sargent, W. L. W. 1996, *ApJ*, 462, 183
- Ho, L. C., Filippenko, A. V., & Sargent, W. L. W. 1997, *ApJS*, 112, 315
- Ishisaki, Y., et al. 1996, *PASJ*, 48, 237
- Jones, M. E. 1991, in *IAU Colloq. 131, Radio Interferometry: Theory, Techniques, and Applications*, ed. T. J. Cornwell & R. A. Perley (San Francisco: ASP), 295
- Kaufman, M., Bash, F. N., Crane, P. C., & Jacoby, G. H. 1996, *AJ*, 112, 1021
- Keel, W. C. 1989, *AJ*, 98, 195
- Kellermann, K. I., & Owen, F. N. 1988, in *Galactic and Extragalactic Radio Astronomy*, ed. G. L. Verschuur & K. I. Kellermann (New York: Springer-Verlag), 563
- Morabito, D. D., Preston, R. A., & Jauncey, D. L. 1988, *AJ*, 95, 1037
- Morris, D. 1991, VLA Test Memorandum No. 182 (National Radio Astronomy Observatory)

- Napier, P. J., & Rots, A. H. 1982, VLA Test Memorandum No. 134 (National Radio Astronomy Observatory)
- Pauliny-Toth, I. I. K., & Kellermann, K. I. 1966, *ApJ*, 146, 634
- Peimbert, M., & Torres-Peimbert, S. 1981, *ApJ*, 245, 845
- Peterson, F. W., & Dent, W. A. 1973, *ApJ*, 186, 421
- Pooley, G. G., & Green, D. A. 1993, *MNRAS*, 264, L17
- Reuter, H.-P., & Lesch, H. 1996, *A&A*, 310, L5
- Shuder, J. M., & Osterbrock, D. E. 1981, *ApJ*, 250, 55
- Slee, O. B., Sadler, E. M., Reynolds, J. E., & Ekers, R. D. 1994, *MNRAS*, 269, 928
- van der Laan, H. 1966, *Nature*, 211, 1131
- Van Dyk, S. D., Weiler, K. W., Sramek, R. A., Rupen, M. P., & Panagia, N. 1994, *ApJ*, 432, L115
- Weiler, K. W., Sramek, R. A., Panagia, N., van der Hulst, J. M., & Salvati, M. 1986, *ApJ*, 301, 790
- Wright, M. C. H., & Backer, D. C. 1993, *ApJ*, 417, 560
- Wrobel, J. M., & Heeschen, D. S. 1991, *AJ*, 101, 148
- Zhao, J.-H., Goss, W. M., Lo, K. Y., & Ekers, R. D. 1992, in *Relationships Between Active Galactic Nuclei and Starburst Galaxies*, ed. A. V. Filippenko (San Francisco: ASP), 295